

Advanced Composite Materials

Publication details, including instructions for authors and subscription information:

<http://www.tandfonline.com/loi/tacm20>

Quantitative Accessibility of Delamination in Composite Using Lamb Wave by Experiments and FEA

Kyoung-Tak Kang ^a, Heoung-Jae Chun ^b, Joo-Hyun Son ^c, Jin-Ah Lee ^d, Joon-Hyung Byun ^e, Moon-Kwang Um ^f, Sang-Kwan Lee ^g & Ju-Woong Jang ^h

^a School of Mechanical Engineering, Yonsei University, 50 Yonsei-Ro, Seodaemun-Gu, Seoul 120-749, Korea

^b School of Mechanical Engineering, Yonsei University, 50 Yonsei-Ro, Seodaemun-Gu, Seoul 120-749, Korea; Email: tagi1024@yonsei.ac.kr

^c School of Mechanical Engineering, Yonsei University, 50 Yonsei-Ro, Seodaemun-Gu, Seoul 120-749, Korea

^d School of Mechanical Engineering, Yonsei University, 50 Yonsei-Ro, Seodaemun-Gu, Seoul 120-749, Korea

^e Korea Institute of Materials Science, 66 Sangnam-Dong, Changwon, Kyungnam 641-010, Korea

^f Korea Institute of Materials Science, 66 Sangnam-Dong, Changwon, Kyungnam 641-010, Korea

^g Korea Institute of Materials Science, 66 Sangnam-Dong, Changwon, Kyungnam 641-010, Korea

^h The Institute of Biomaterial & Medical Engineering, Korea Bone Bank Co. Ltd, Ace Techno Tower 9th 402, Gasan-Dong, Geumcheon-Gu, Seoul 153-802, Korea

Version of record first published: 02 Apr 2012.

To cite this article: Kyoung-Tak Kang, Heoung-Jae Chun, Joo-Hyun Son, Jin-Ah Lee, Joon-Hyung Byun, Moon-Kwang Um, Sang-Kwan Lee & Ju-Woong Jang (2011): Quantitative Accessibility of Delamination in Composite Using Lamb Wave by Experiments and FEA, *Advanced Composite Materials*, 20:4, 361-373

To link to this article: <http://dx.doi.org/10.1163/092430411X558503>

PLEASE SCROLL DOWN FOR ARTICLE

Full terms and conditions of use: <http://www.tandfonline.com/page/terms-and-conditions>

This article may be used for research, teaching, and private study purposes. Any substantial or systematic reproduction, redistribution, reselling, loan, sub-licensing, systematic supply, or distribution in any form to anyone is expressly forbidden.

The publisher does not give any warranty express or implied or make any representation that the contents will be complete or accurate or up to date. The accuracy of any instructions, formulae, and drug doses should be independently verified with primary sources. The publisher shall not be liable for any loss, actions, claims, proceedings, demand, or costs or damages whatsoever or howsoever caused arising directly or indirectly in connection with or arising out of the use of this material.

Quantitative Accessibility of Delamination in Composite Using Lamb Wave by Experiments and FEA

Kyoung-Tak Kang^a, Heoung-Jae Chun^{a,*}, Joo-Hyun Son^a, Jin-Ah Lee^a,
Joon-Hyung Byun^b, Moon-Kwang Um^b, Sang-Kwan Lee^b and Ju-Woong Jang^c

^a School of Mechanical Engineering, Yonsei University, 50 Yonsei-Ro, Seodaemun-Gu, Seoul 120-749, Korea

^b Korea Institute of Materials Science, 66 Sangnam-Dong, Changwon, Kyungnam 641-010, Korea

^c The Institute of Biomaterial & Medical Engineering, Korea Bone Bank Co. Ltd, Ace Techno Tower 9th 402, Gasan-Dong, Geumcheon-Gu, Seoul 153-802, Korea

Received 24 August 2010; accepted 3 January 2011

Abstract

Delamination in composite structures plays a major role in lowering structural strength and stiffness, consequently downgrading system integrity and reliability. The aim of this study was to show that Lamb waves may be effectively generated using piezoelectric actuators embedded within a composite plate for use in health monitoring applications. A Lamb wave-based quantitative identification technique for delamination in VARTM (vacuum assisted resin transfer molding) composite structures was established. The propagation of Lamb waves in composite plates was evaluated using dynamic FEM analysis, then an experiment was carried out to verify the validity of the analytical study. The study assessed damage in the plates by fusing information from multiple sensing paths of the embedded network. To eliminate interference, a wavelet transform technique was applied to purify the acquired Lamb wave signals. The results showed that satisfactory detection of defects could be achieved with the proposed method.

© Koninklijke Brill NV, Leiden, 2011

Keywords

Finite element analysis, health monitoring, wavelet transform

1. Introduction

Composite materials are widely used in high-performance structures due to their high specific strength and stiffness coupled with their cost effectiveness over traditional materials [1]. When the composite material structures are damaged, the appearance is unaffected. However, internal damage such as microcracks and delaminations are generated and can eventually cause catastrophic failures of the

* To whom correspondence should be addressed. E-mail: tagi1024@yonsei.ac.kr

Edited by KSCM

structures. Therefore, composite structures must be examined frequently. One of the disadvantages of the current inspection techniques is that the structures have to be taken out of service for inspection, making these techniques inconvenient and inefficient. Furthermore, they are not suitable for structures that are currently in service.

Non-destructive evaluation (NDE) techniques based on Lamb wave propagation have been the subject of study for several decades. Lamb waves, the elastic waves in plate-like structures, can propagate over a relatively long distance, even in materials with high attenuation ratios, allowing for a broad inspection area using only a few transducers. For this reason, structural health monitoring (SHM) techniques have been introduced to provide up-to-the minute condition surveillance [2, 3]. In many current applications, signals are collected using surface bonding or attached transducers, e.g., wedge-coupled ultrasonic probes [4, 5], because of their convenience in attachment, maintenance and replacement. However, these approaches can be inefficient in aerospace applications because they normally require vehicle downtime and incur excessive maintenance costs. Moreover, with sensors directly exposed to the working environment, the capture of signals can be severely compromised by noise from a variety of sources; therefore the reliability and repeatability of signal acquisition may be inadequate.

Isolated from the ambient environment, embedded sensors may offer outstanding stability in the generation and acquisition of interrogative signals, even in rugged environments, as well as high sensitivity to structural damage. It has been demonstrated [6] that embedded PZTs accurately detected cracks as small as 0.1 mm. Lin and Yuan [7, 8] studied Lamb wave propagation in plates integrated with piezoelectric sensor/actuators analytically and experimentally, employing the Mindlin plate theory and considering the effects of transverse shear and rotary inertia in the host plates. PZT disk actuators were mounted symmetrically onto the surfaces of the plates, the piezoelectric effect of the disks was introduced as an equivalent bending moment, and thus the A_0 mode of a Lamb wave was generated and collected. Grondel *et al.* [9] extended the coupled finite element-normal expansion method and developed an experimental technique to optimally generate the A_0 mode of a Lamb wave in a composite plate using surface-bonded piezoceramic transducers, which were also used for damage detection. On the basis of such observations, Lamb waves, including symmetric (S_0) and anti-symmetric (A_0) modes, have been widely exploited for nondestructive evaluation [10, 11].

The aim of the present study was to assess the utility of S_0 and A_0 modes for the quantitative identification of delamination in composite plates. A practical and effective real-time damage identification approach was developed for woven-glass/phenol composite plates. The feasibility of this system was verified by application to the plates for detection of known localized damage. Comparisons between experimental and numerical studies of damage detection were made. Then, an experiment was carried out to verify the validity of the analytical study based on finite element models. A feasibility study was carried out to locate and gauge, based on

the wavelet transform, damage in VATRM composites using data from the multiple sensing paths in the embedded network.

2. Delamination in Composite Plates

Laminated composite structures are highly susceptible to low-velocity impact, resulting in invisible damage which manifests itself as fibre breakage, matrix cracking, or local delaminating [12]. In particular, delamination appearing as the debonding of adjoining plies is the most hazardous defect for laminated composites and can be induced during careless manufacture or as a consequence of accidental impact. The occurrence of delamination considerably lowers structural strength and stiffness and severely reduces structural integrity. Both theoretical studies [13, 14] and numerical simulations [4, 15] focusing on delamination in carbon fiber-reinforced composite laminates and in which one- or two-dimensional assumptions were applied during modeling have been well-developed. This study, however, aimed at a higher simulation precision, so a three-dimensional full-scale FEM modeling technique was developed.

3. Procedure for Evaluating Delamination

In non-destructive evaluation (NDE), a common understanding is that the ultrasonic scanning technique can usually detect damage with a characteristic size larger than one-half of the wavelength of the ultrasonic wave. Successful Lamb wave generation and acquisition are key prerequisites for a practical damage detection technique. It has been observed that a higher algebraic product of frequency and plate thickness is associated with more significant dispersion phenomena and more multiple wave modes [16].

Usually a relatively low frequency is preferable where only two fundamental modes, namely the S_0 and A_0 modes, are available. For this reason, the fundamental A_0 mode is preferable and more sensitive to damage because its wavelength is shorter than that of the S_0 mode at the same frequency. However, the A_0 mode exhibits more severe dispersion at low frequencies, and more stringent experimental configurations are normally required to prevent energy leakage from its substantial out-of-plane vibrations. In contrast, the shape of the S_0 mode is simple and the stresses it causes are almost uniform throughout the thickness of the plate at small products of frequency and plate thicknesses up to $1 \text{ MHz} \cdot \text{mm}$ [17]. Additionally, for application in the excitation mechanism of a piezoelectric (PZT) actuator, the S_0 mode always exists in the actuated Lamb waves. To excite the A_0 mode solely at low frequencies, some specific method, such as dual actuators with reverse phase actuation, is required [18]. In this study, PZT actuators were embedded within a composite plate to actuate Lamb waves wherein both S_0 and A_0 modes were generated synchronously. Therefore, unlike in the previous studies, we excited two modes for quantitative evaluation and comparison since both S_0 and A_0 modes have advantages and disadvantages in defect scanning.

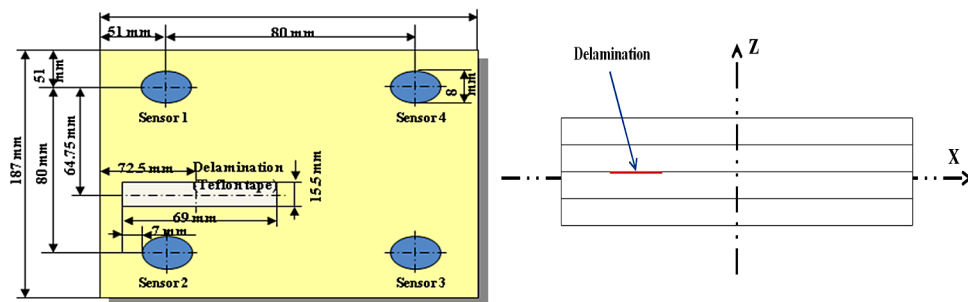


Figure 1. Specimen configurations in the FEM and experiment. This figure is published in color in the online version.

Table 1.

Material properties of the VARTM specimen

E_{11} (GPa)	E_{22} (GPa)	E_{33} (GPa)	G_{12} (GPa)	ν_{12}	ν_{21}	ρ (g/cm ³)
20	20	5	2.49	0.08	0.08	2.00

3.1. Explicit Dynamic Analysis Using FEM

Explicit dynamic analysis is computationally efficient for the analysis of large models with relatively short dynamic response times and is ideally suited for analyzing high-speed dynamic events [19]. A four-ply VARTM composite plate with dimensions $0.187 \times 0.187 \times 0.019$ m³ was considered and is shown in Fig. 1. The mechanical properties of the plate are listed in Table 1. The effective material properties of the whole composite plate are considered using the laminate plate theory. In the delaminated region, a volume-split was formed by separating two delamination surfaces by a distance of one-half the thickness of an individual lamina, as illustrated in Fig. 2. For accurate simulation of wave propagation, the model was finely meshed using eight-node 3-D brick elements, with four layers of elements in the plate thickness corresponding to the four laminates. At least ten elemental nodes were allocated within the Lamb wave wavelength to guarantee the validity of the simulated dynamic responses. This mesh density led to approximately 30 000 elements in total for the delaminated plate. A surface contact algorithm [19] was introduced to process the contact problem arising from delamination by primarily relaxing the restrictions on the two contactable surfaces. The contact algorithm permits a small relative sliding displacement and an arbitrary rotation of the two delaminated surfaces. Both the upper and lower delamination surfaces were defined using an element-based deformable surface [19], allowing interaction between the two surfaces in the normal direction, but resisting mutual penetration. A full-scale FEM model for the VARTM specimen was created using the HYPERMESH platform.

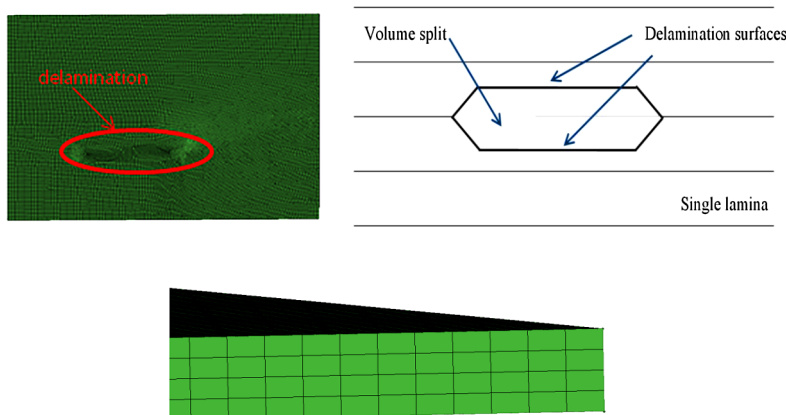


Figure 2. Modeling of delamination. This figure is published in color in the online version.

3.2. FEM Simulation

A Lamb wave was numerically generated in the delaminated plate. A previous study [20] verified that a Lamb wave with a waveform of five-cycle sinusoid tone bursts windowed by the Hanning function can benefit the signal identification. It also effectively prevents wave dispersion and makes the signal interpretation explicit. In this study, PZT disc transducers were chosen as transmitters and receivers since they exhibit simultaneous actuator and sensor behaviors. The Lamb wave was activated at a central frequency of 0.265 MHz by evenly applying a horizontal displacement at all of the nodes across the thickness of the plate, as illustrated in Fig. 3. The generated Lamb wave with its frequency spectrum determined *via* fast Fourier transform (FFT) is also exhibited in Fig. 3. A majority of its energy was observed to centralize around 0.265 MHz. Lamb wave propagation in the delaminated laminate was simultaneously monitored at a sampling rate of 20.48 MHz. The dynamic simulation was conducted using ABAQUS/Explicit with a time step for dynamic calculation that was less than the ratio of the minimum distance between any two adjoining nodes to the maximum Lamb wave velocity in the excitation frequency range. Due to the absence of an element type with piezoelectric function in ABAQUS/Explicit, a specific modeling technique for the PZT actuator model and sensor has been introduced [21]. In the actuator model, a uniform radial displacement in the x – y plane was applied to all nodes along the edge of the actuator in order to generate the fundamental symmetric and anti-symmetric Lamb wave modes. The actuation case was applied to study the interaction of the Lamb wave modes with a delamination. A single PZT actuator embedded within the plate was simulated by applying both a shear force and a bending moment to generate the S_0 and A_0 modes simultaneously [22].

3.3. Experimental Characterization

A specimen with the same geometry, mechanical properties, and boundary conditions as those in the FEM simulation was experimentally evaluated. Figure 4

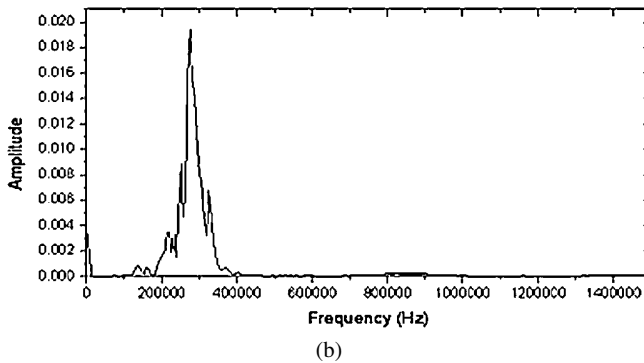
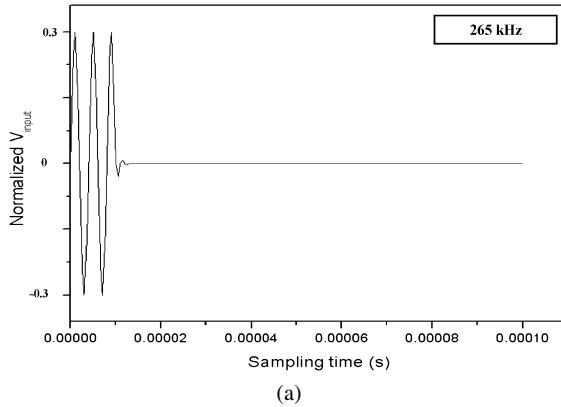


Figure 3. Input excitation signals in the (a) time domain, (b) frequency domain.

illustrates the active real-time structural health monitoring system developed in this study. In this system, PZT disc transducers with a circular shape (Kyungwon Inc.) were chosen as transmitters and receivers since they can exhibit simultaneous actuator and sensor behaviors. Transducer arrays in each region were used to measure the group velocity. A function generator (Ram-10000, Ritec) was used to excite the transmitting actuators. The applied excitation signal was five cycles of a 0.265 MHz sinusoidal tone burst enclosed in a Hanning window. The received signals were collected with a digital oscilloscope (CS225, Gage Inc.). The validity of this system was studied using a four-layer woven-glass/phenol laminate plate with predetermined delamination. Teflon tape with a length of 69 mm and width of 15.5 mm was inserted between the second and third layers to simulate common delamination. The center of the delamination was 72.5 mm from the left and bottom edges of the plate. The received signals were acquired at a sampling rate of 2.0 MS/s by the oscilloscope, which averaged 32 samples, to improve the S/N ratio. The central frequency of the transmitting signal was 0.265 MHz. However, the central frequencies of the received signals when Lamb waves were propagated within each region did not correspond to this value. In other words, there was a deviation from the central frequency of the transmitting signal. All signal analyses were performed on the MatLab Platform.

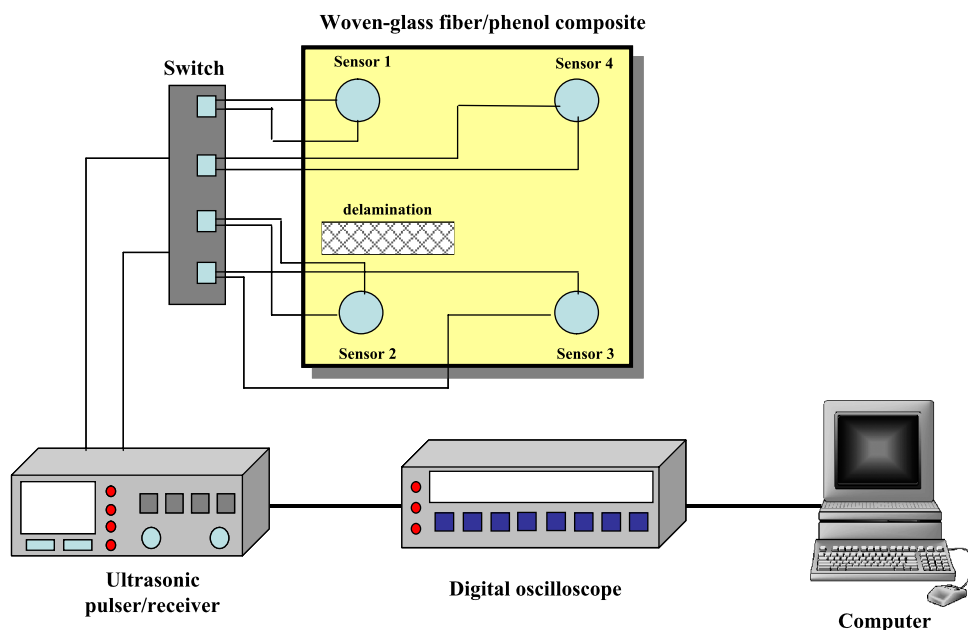


Figure 4. Schematic drawing of the experimental setup. This figure is published in color in the online version.

4. Wavelet Transform

It can be concluded that an embedded PZT sensor, protected from the environment, allows for excellent immunity to environmental noise delivering an enhanced signal-to-noise ratio (SNR) and a steady amplitude output. However, an embedded PZT sensor normally generates both symmetrical and anti-symmetrical wave modes simultaneously. Meanwhile, mode reflection occurs at boundaries, discontinuities, or structural defects, resulting in a complicated multimode wave signal. Furthermore, other sources of interference, for example material attenuation, natural structural vibration, and experimental broadband noise, also inevitably deteriorate the wave signal and obscure the signal characteristics. For this reason, appropriate signal processing methods must be applied to wave signals in order to distinguish and extract the characteristic information. Advanced signal processing algorithms combining time, space, and frequency information, such as the short time Fourier transform (STFT), two-dimensional Fourier transform (2DFT), and wavelet transform (WT), have been applied extensively for signal processing in structural health monitoring. In this study, the WT technique was adopted to process the acquired wave signals. The WT is an important linear time–frequency representation of signals which maps a one-dimensional time signal into a two-dimensional function of time and frequency. In contrast to the STFT, the WT automatically scales the time window function to cover both high-frequency and low-frequency signal resolutions [23].

A continuous wavelet transform (CWT) of a signal can be written as [24]:

$$(W_{\psi})(a, b) = \frac{1}{\sqrt{a}} \int_{-\infty}^{\infty} x(t) \psi^* \left(\frac{t-b}{a} \right) dt, \quad (1)$$

where a , b , $\Psi(t)$ and Ψ^* are the scale parameter, time shift, basic wavelet, and complex conjugate of Ψ^* , respectively. The CWT is then correspondingly simplified as the discrete wavelet transform (DWT), and the original signal can be reconstructed from the wavelet synthesis formulas using [24]:

$$x_m(t) = \sum_{n=-\infty}^{+\infty} a_k \psi_{m,n}(t), \quad (2)$$

where n , m and a_k are the dyadic time-scale integers and the wavelet amplitude, respectively. Unlike the CWT, which operates at every scale and over a continuous time shift across the full domain of the analyzed signal, the DWT decomposes and rebuilds the signal at separate levels of frequencies with multi-resolution analysis using the Matlab algorithm to reduce redundant coefficients of equal magnitude [25]. The notion of scale or level in the WT is proportional to its reciprocal and is a substitute for frequency. Each scale or level in the time-scale domain corresponds to a certain region of frequencies in the time–frequency domain. In this work, both the DWT and the CWT were performed successively to extract the characteristics of the acquired Lamb wave signals.

5. Results

In the numerical and experimental studies, the group velocities of the Lamb wave modes excited by PZT sensors in the signals from the specimens without delamination were determined by calculating the time of flight between a pair of transducers at a certain distance. As the fastest mode, the S_0 mode arrived prior to all available Lamb wave modes in the time sequence. The theoretical dispersion curves for the group velocity were derived using the formalism of Nayfeh [26]. The dispersion curves in Fig. 5 show that there can be two modes (S_0 , A_0) at 0.265 MHz. The group velocities were 3.2 km/s for the S_0 mode, and 1.1 km/s for the A_0 mode at a center frequency of 0.265 MHz. The group velocities of only two Lamb wave modes could be detected in the specimens without delamination because they are non-dispersive in this range.

The procedure for the feature extraction from the Lamb wave signals is explained. First, the raw signals were decomposed into multiple frequency regions *via* the DWT, and the relevant level comprising the excited frequency of 0.265 MHz was selected to filter the noise from other frequency bands. Second, wavelet coefficients were calculated in the time-scale domain *via* the CWT from the purified signals. Then, the energy spectrum based on the wavelet coefficients was integrated along the scale axis to construct the energy profile in the time domain for feature extraction and damage assessment. This procedure ensures that the wave signal and

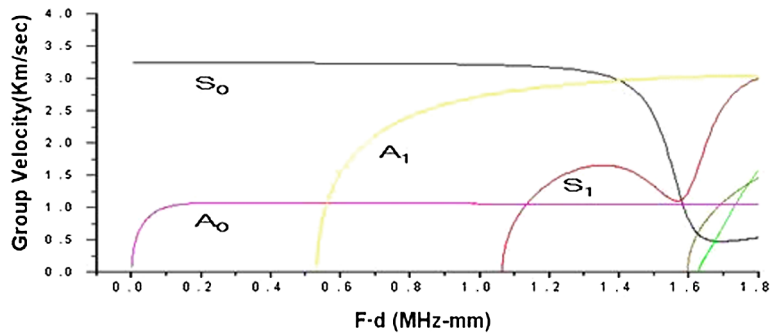


Figure 5. Dispersion curves for group velocity in the VARTM specimen. This figure is published in color in the online version.

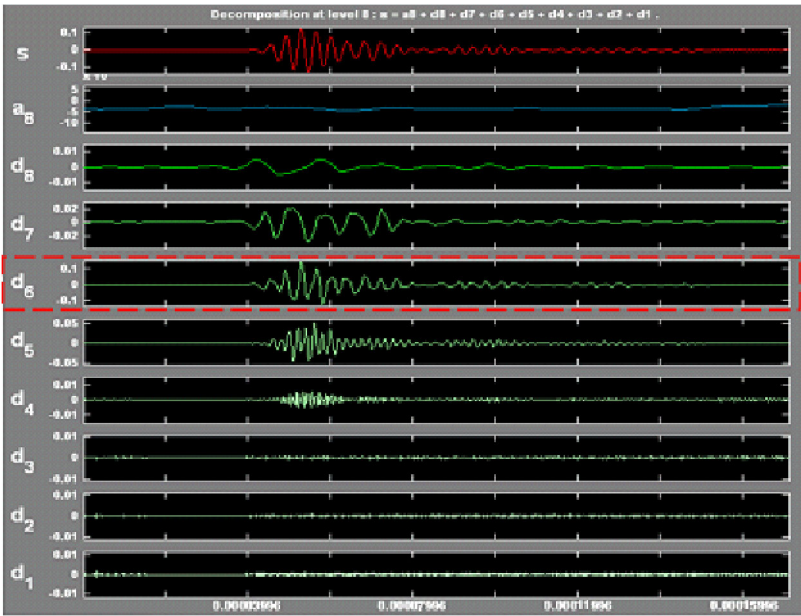


Figure 6. Multiple resolution of the DWT analysis of signals along the delamination path. This figure is published in color in the online version.

its corresponding energy distribution in the time domain were concentrated in a narrower band of the excited frequency after the WT analysis so as to enhance the wave scattering for defect detection. Using a Daubechies wavelet, the raw wave signals were decomposed into eight levels corresponding to the frequency regions. The chosen sampling frequency of 20.48 MHz provided an effective sampling range up to 10.24 MHz based on the Nyquist sampling theory [27]. It can therefore be observed in Fig. 6 that the main components of the source wave signal were focused in a detailed part of Level 6. The analytical results from DWT at the 6th Level are shown in Fig. 7.

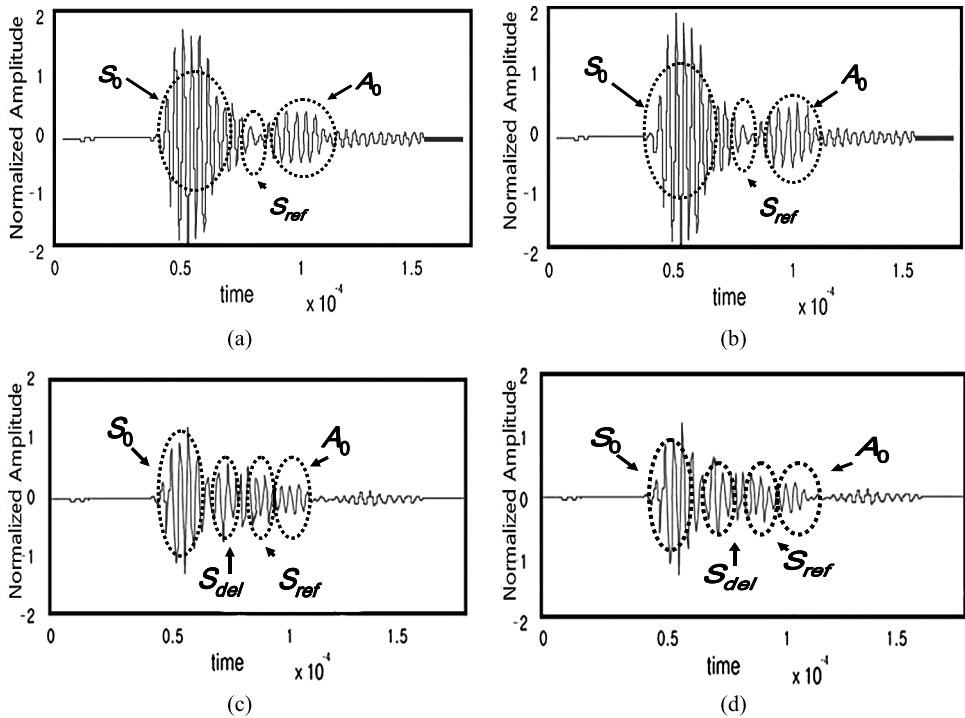


Figure 7. CWT analysis of signals on plates without and with delamination: (a) FEM (without delamination), (b) experimental (without delamination), (c) FEM (with delamination), (d) experimental (with delamination).

Figure 7 shows DWT analysis signals from plates with and without delamination. Good correlation between the numerical and experimental results was observed for the incipient S_0 and A_0 modes with the discrepancy in propagation velocity being less than 5%. In the figure, the two modes are clearly identified as the S_0 and A_0 modes. The normal displacement amplitude of the S_0 mode was in fact twice as large as that of the A_0 mode. This quantitative result is in agreement with the theory, as indicated in Fig. 5. However, when delamination existed in the Lamb wave paths, the signals showed significant changes (Fig. 7). Therefore, it is possible to judge the presence of internal defects by monitoring the changes in the received signals. It is noted in Fig. 7 that the extra wave packet induced by the delamination, defined as S_{del} , can be clearly observed between the incipient wave packet (S_0) and the wave packet reflected from the boundary (S_{ref}) in the wavelet-reconstructed signals.

After being normalized to the maximum amplitude of the incipient wave packet in the plate without delamination, the amplitude of the incipient wave packet in the delaminated plates can be seen to decrease. It is believed that more incident waves were scattered at the delamination site, contributing to greater dissipation of wave energy. Similar characteristics were also observed in the distribution of wavelet coefficients in the time-scale domain in the CWT analysis (Fig. 8). The extra strip

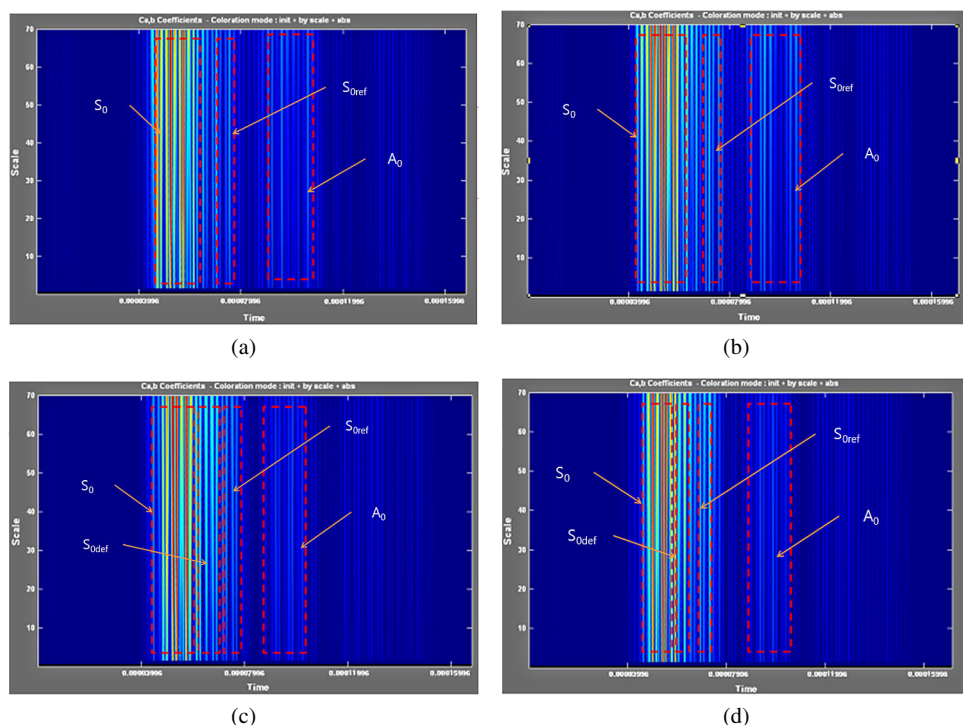


Figure 8. 2D CWT spectra signals from plates without and with delamination: (a) FEM (without delamination), (b) experimental (without delamination), (c) FEM (with delamination), (d) experimental (with delamination). This figure is published in color in the online version.

of energy density induced by the delamination is emphasized between the S_0 and S_{ref} parts, and the blue scales in Fig. 8(c) and 8(d) represent the greater amount of energy scattered with the increase in delamination. Thus, even if the sensor is lower than the selected cut-off frequency, the center frequency appropriate to each specimen should be determined experimentally. The results also showed that the S_0 mode was more effective than the A_0 mode at detecting delamination.

6. Conclusions

Delamination is a common type of damage widely found in advanced composite structures. In this study, an embeddable active PZT sensor network was developed to increase the functionality and reliability of damage assessment and to monitor the conditioning of the composite structures. The propagation characteristics of Lamb waves generated and collected by the embedded sensor network were numerically and experimentally evaluated. The analytical results of the numerical study using finite element models showed successful damage prediction consistent with the trends in the experimental study. Numerical and experimental investigations showed that the S_0 mode was dominant over the A_0 mode during propagation in a VARTM specimen. The embedded sensor network had an immunity to environmen-

tal noise, excellent stability, and repeatability in data acquisition when compared with traditional surface-bonded PZT sensors. The generated wave exhibited non-dispersive properties under an excitation frequency of 0.265 MHz in the VARTM specimen. A feasibility study was conducted using the embedded sensor network for detection of damage in the VARTM specimen on the basis of wavelet transform. It was shown that good diagnostic results can be achieved with this method. The wavelet transform method can be used for the detection of delamination in composite plates. Its excellent identification capabilities show significant potential for improving the integrity of composite structures. Further studies will focus on the development of identification techniques for the extent of delamination.

Acknowledgements

This research was supported by a grant from the Center for Advanced Materials Processing (CAMP) of the 21st Century Frontier R and D Program funded by the Ministry of Science and Technology, Republic of Korea and by the Aerospace Material Technology Development funded by the Ministry of Knowledge Economy, Republic of Korea.

References

1. I. M. Daniel and O. Ishai, *Engineering Mechanics of Composite Materials*. Oxford University Press, New York, USA (1994).
2. M. Lin and F. K. Chang, The manufacture of composite structures with a built-in network of piezoceramics, *Compos. Sci. Technol.* **62**, 919–939 (2002).
3. H. Fukunaga, N. Hu and F. K. Chang, Structural damage identification using piezoelectric sensors, *Intl J. Solids Struct.* **39**, 393–418 (2002).
4. N. Guo and P. Cawley, Lamb waves for the NDE of composite laminates, *Rev. Prog. Quantit. Nondestruct. Eval.* **11**, 1443–1450 (1992).
5. F. L. Degertekin and B. Khuri-Yakub, Lamb wave excitation by Hertzian contacts with applications in NDE, *IEEE Trans. Ultrasonics, Ferroelect. Freq. Control* **44**, 769–779 (1997).
6. Y. J. Yan and L. H. Yam, Online detection of crack damage in composite plates using embedded piezoelectric actuators/sensors and wavelet analysis, *Compos. Struct.* **58**, 29–38 (2002).
7. X. Lin and F. G. Yuan, Diagnostic Lamb waves in an integrated piezoelectric sensor/actuator plate: analytical and experimental studies, *Smart Mater. Struct.* **10**, 907–913 (2001).
8. X. Lin and F. G. Yuan, Detection of multiple damages by prestack reverse-time migration, *AIAA J.* **39**, 2206–2224 (2001).
9. S. Grondel, C. Paget, C. Delebarre, J. Assaad and K. Levin, Design of optimal configuration for generating a Lamb mode in a composite plate using piezoceramic transducers, *J. Acoust. Soc. Amer.* **112**, 84 (2002).
10. D. N. Alleyne and P. Cawley, The interaction of Lamb waves with defects, *IEEE Trans. Ultrasonics, Ferroelect. Freq. Control* **39**, 381–397 (1992).
11. C. S. Wang and F. K. Chang, Built-in diagnostics for impact damage identification of composite structures, in: *Structural Health Monitoring 2000*, F. K. Chang (Ed.), pp. 612–621. Technomic Pub., Lancaster, PA (2000).

12. A. S. Islam and K. C. Craig, Damage detection in composite structures using piezoelectric materials, *Smart Mater. Struct.* **3**, 318–328 (1994).
13. P. M. Mujumdar and S. Suryanarayan, Flexural vibrations of beams with delaminations, *J. Sound Vibr.* **125**, 441–461 (1988).
14. W. Ostachowicz, M. Krawczuk, M. P. Cartmell and M. Gilchrist, Detection of delaminations using spectral finite element, in: *Proc. 1st European Workshop on Structural Health Monitoring*, Paris, France, pp. 10–12. DEStech (2002).
15. N. Guo and P. Cawley, Lamb wave propagation in composite laminates and its relationship with acousto-ultrasonics, *NDT and E Intl* **26**, 75–84 (1993).
16. D. Alleyne and P. Cawley, Optimization of Lamb wave inspection techniques, *NDT and E Intl* (1992).
17. M. J. S. Lowe and O. Diligent, Low-frequency reflection characteristics of the s Lamb wave from a rectangular notch in a plate, *J. Acoust. Soc. Amer.* **111**, 64 (2002).
18. Z. Su and L. Ye, Selective generation of Lamb wave modes and their propagation characteristics in defective composite laminates, *Proc. Institution of Mech. Engrs, Part L: J. Mater.: Design Appl.* **218**, 95–110 (2004).
19. I. Abaqus, Abaqus User's Manual, Version 6 (2003).
20. S. S. Kessler, S. M. Spearing and C. Soutis, Damage detection in composite materials using Lamb wave methods, *Smart Mater. Struct.* **11**, 269–278 (2002).
21. Z. Su and L. Ye, Lamb Wave propagation-based damage identification for quasi-isotropic CF/EP composite laminates using artificial neural algorithm: Part I. Methodology and database development, *J. Intelligent Mater. Syst. Struct.* **16**, 97 (2005).
22. C. Yang, L. Ye, Z. Su and M. Bannister, Some aspects of numerical simulation for Lamb wave propagation in composite laminates, *Compos. Struct.* **75**, 267–275 (2006).
23. M. Misiti, Y. Misiti, G. Oppenheim and J. M. Poggi, *Wavelet Toolbox User's Guide, Version 2.1*, The MathWorks Inc., Natick, MA, USA (2000).
24. W. J. Staszewski, C. Boller and G. R. Tomlinson, *Health Monitoring of Aerospace Structures: Smart Sensor Technologies and Signal Processing*. Wiley, New York, NY (2004).
25. M. Lemistre and D. Balageas, Structural health monitoring system based on diffracted Lamb wave analysis by multiresolution processing, *Smart Mater. Struct.* **10**, 504–511 (2001).
26. A. H. Nayfeh, The general problem of elastic wave propagation in multilayered anisotropic media, *J. Acoust. Soc. Amer.* **89**, 1521 (1991).
27. MathWorks, *6.1 Signal Processing Toolbox Documentation*, MathWorks Inc., Natick, MA, USA (2001).